Accepted Manuscript

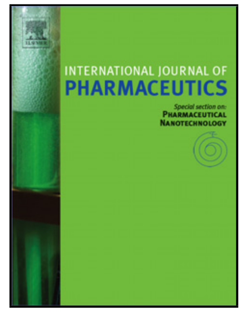

Title: Unexpected solvent impact in the crystallinity of Praziquantel/**Poly(vinylpyrrolidone) formulations. A Solubility, DSC and Solid-State NMR study**

Author: Emanuel D. Costa Josefina Priotti Silvina Orlandi Darío Leonardi María C. Lamas Teresa G. Nunes Hermínio P. Diogo Claudio J. Salomon M. João Ferreira

PII: S0378-5173(16)30738-4
DOI: http://dx.doi.org/doi:10.1016/j.ijpharm.2016.08.009
Reference: IJP 15985

To appear in: *International Journal of Pharmaceutics*

Received date: 20-6-2016
Revised date: 3-8-2016
Accepted date: 5-8-2016

Please cite this article as: Costa, Emanuel D., Priotti, Josefina, Orlandi, Silvina, Leonardi, Darío, Lamas, María C., Nunes, Teresa G., Diogo, Hermínio P., Salomon, Claudio J., Ferreira, M.João, Unexpected solvent impact in the crystallinity of Praziquantel/Poly(vinylpyrrolidone) formulations.A Solubility, DSC and Solid-State NMR study.International Journal of Pharmaceutics http://dx.doi.org/10.1016/j.ijpharm.2016.08.009

This is a PDF file of an unedited manuscript that has been accepted for publication. As a service to our customers we are providing this early version of the manuscript. The manuscript will undergo copyediting, typesetting, and review of the resulting proof before it is published in its final form. Please note that during the production process errors may be discovered which could affect the content, and all legal disclaimers that apply to the journal pertain.

ACCEPTED MANUSCRIPT

Unexpected solvent impact in the crystallinity of Praziquantel/Poly(vinylpyrrolidone) formulations. A Solubility, DSC and Solid-State NMR study

Emanuel D. Costa,[a] *Josefina Priotti,*[b,c] *Silvina Orlandi,*[c] *Darío Leonardi,*[b,c] *María C. Lamas,*[b,c] *Teresa G. Nunes,*[a] *Hermínio P. Diogo,*[a] *Claudio J. Salomon,*[b,c*] *M. João Ferreira*[a*]

[a]CQE, Instituto Superior Técnico, Universidade de Lisboa, Av. Rovisco Pais, 1049-001 Lisboa, Portugal

[b]IQUIR-CONICET, Suipacha 531, 2000. Rosario, Argentina.

[c]Área Técnica Farmacéutica, Facultad de Cs. Bioquímicas y Farmacéuticas, Universidad Nacional de Rosario, Suipacha 531, 2000. Rosario, Argentina.

Corresponding Authors:

E-mail address: csalomon@fbioyf.unr.edu.ar (C.J. Salomon)

E-mail address: m.joao.ferreira@tecnico.ulisboa.pt (M.J. Ferreira)

ACCEPTED MANUSCRIPT

Graphic Abstract

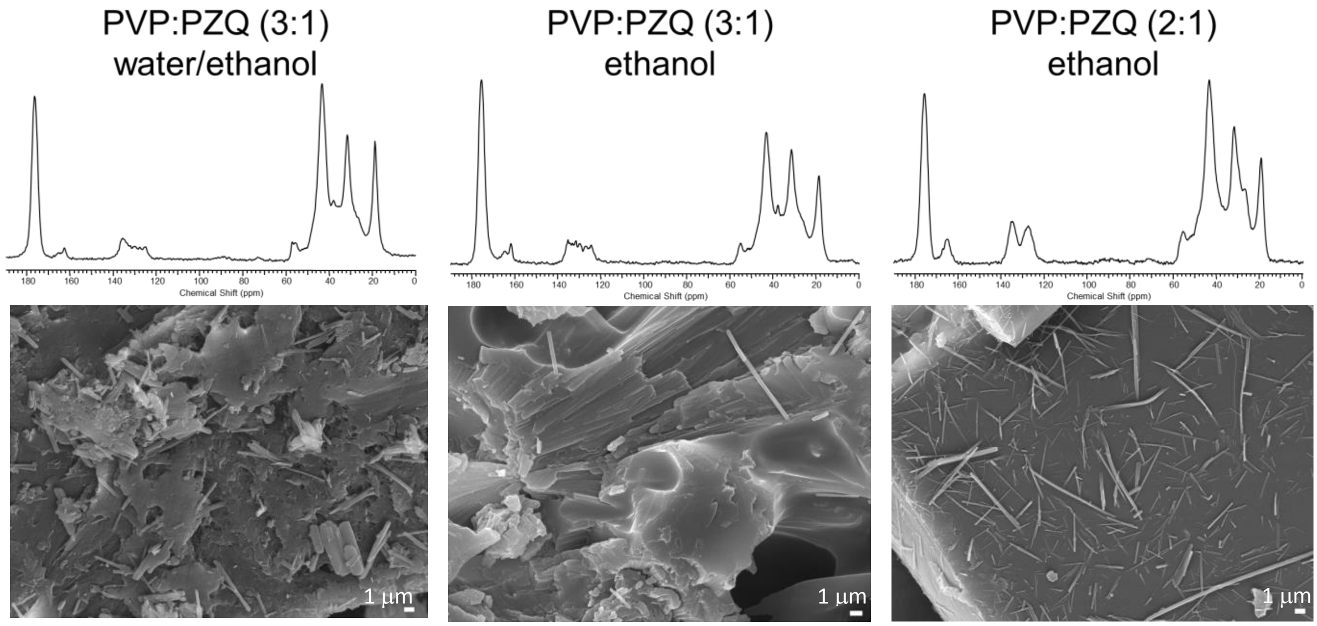

ACCEPTED MANUSCRIPT

ABSTRACT

The saturation solubility of PVP:PZQ physical mixtures (PMs) and solid dispersions (SDs) prepared from ethanol (E/E) or ethanol/water (E/W) by the solvent evaporation method at 1:1, 2:1 and 3:1 ratio (w/w) was determined. The presence of PVP improves the solubility of PZQ (0.31±0.01 mg/mL). A maximum of 1.29±0.03 mg/mL of PZQ in solution was achieved for the 3:1 SD (E/E). The amount of PZQ in solution depends on the amount of polymer and on the preparation method. Solid-state NMR (ssNMR) and DSC were used to understand this behavior. Results show that PMs are a mixture of crystalline PZQ with the polymer, while SDs show different degrees of drug amorphization depending on the solvent used. For E/W SDs, PZQ exists in amorphous and crystalline states, with no clear correlation between the amount of crystalline PZQ and the amount of PVP. For E/E SDs, formulations with a higher percentage of PZQ are amorphous with the components miscible in domains larger than 3 nm (^{1}H ssNMR relaxation measurements). Albeit its higher saturation solubility, the 3:1 E/E PVP:PZQ sample has a significant crystalline content, probably due to the water introduced by the polymer. High PVP content and small crystal size account for this result.

Abbreviations

PZQ, Praziquantel; PVP, Poly(vinylpyrrolidone); NMR, Nuclear Magnetic Resonance; DSC, Differential Scanning Calorimetry; SEM, Scanning Electron Microscopy; PMs, Physical Mixtures; SDs, Solid Dispersions.

KEYWORDS: Praziquantel, Poly(vinylpyrrolidone), solid-state NMR, DSC, pharmaceutical formulations

ACCEPTED MANUSCRIPT

1. INTRODUCTION

Schistosomiasis is an acute and chronical parasitic disease caused by trematode worms of the genus *Schistosoma*. The infection exists in tropical and sub-tropical areas, affecting mainly poor communities with no access to potable water and sanitation. According to the World Health Organization (WHO), there are close to 240 million people in the world infected, several million of which suffer from severe morbidity, in an area where around 700 million people live.(WHO, 16a) The disease has been fought successfully with anthelminthic drugs, with Praziquantel (PZQ), 2-(Cyclohexylcarbonyl)-1,2,3,6,7,11b-hexahydro-4H-pyrazino[2,1-a]isoquinolin-4-one, as the recommended treatment against all forms of schistosomiasis (Fig. 1).

Fig.1 here

PZQ exists commercially as a racemic compound, with two isomers (*R* and *S* enantiomers). Studies have revealed that only the enantiomer *R* has therapeutic value, with the *S* enantiomer being only responsible for the bad taste associated with the drug.(Meyer et al, 2009) Although the WHO and the Center for Disease Control (CDC) consider PZQ an effective, safe and low-cost drug,(CDC, 12); (WHO, 16b) this is far from being a perfect drug, mainly because of its low solubility in water (only 0.04 g/100 mL)(de la Torre et al, 1999); (El-Arini et al, 1998) and a first pass effect(Lindenberg et al, 2004) that compromises its bioavailability. In fact, PZQ is classified in the Biopharmaceutical Classification System (BCS) as a type II drug (poorly soluble, highly permeable).(Lindenberg et al, 2004)

Attaining a better bioavailability can be economically achieved by the appropriate pharmaceutical formulations that help dissolve PZQ in water, improving its effectiveness. Several strategies have been reported in the literature, such as the encapsulation in cyclodextrin derivatives,(Arrúa et al, 2015); (Chaves et al, 2010) the use of water soluble polymers such as

ACCEPTED MANUSCRIPT

PVP(Baghel et al, 2016); (de la Torre et al, 1999); (Trastullo et al, 2015) and poly(ethyleneglycol),(Bagade et al, 2015); (Passerini et al, 2006) inclusion in poly(methyl metacrylate) nanoparticles,(Fonseca et al, 2013); (Malhado et al, 2016) liposome encapsulation(Frezza et al, 2013) and even complexation to metal centers.(Patra et al, 2013)

PVP:PZQ formulations have attracted the attention of several research groups. PVP has been extensively used as an excipient in several pharmaceutical formulations mostly as a tablet binder and bioavailability enhancer and is considered safe.(Haaf et al, 1985) Given the molecular structures of both PVP and PZQ (Fig. 1), one expects that the interactions between the two molecules to be mostly van der Waals forces that should be strong enough to promote drug dissolution but weak enough to allow its release. And indeed it has been demonstrated that an increase in the amount of PVP increases PZQ solubility and that physical mixtures and solid dispersions behave differently in terms of solubility and dissolution rates.(El-Arini et al, 1998) Furthermore, amorphous PZQ inclusion in the PVP matrix has been demonstrated by scanning electron microscopy (SEM) and X-ray powder diffraction (DRX).(de la Torre et al, 1999)

The development of amorphous solid dispersions is of great interest, so it is crucial to find suitable techniques to characterize them in terms of drug degradation, crystallinity of the active principle, drug-carrier miscibility and intermolecular interactions. Common techniques include thermal analysis and X-ray diffraction, (Baird and Taylor, 2012); (LaFountaine et al, 2016) but these can have some limitations in differentiating between amorphous and crystalline phases and in obtaining further information if specific thermal events are not well resolved, when for instance the drug and the polymer mixture having similar *Tg* values.(Newman et al, 2008); (Tatton et al, 2013) Solid-state Nuclear Magnetic Resonance (ssNMR) spectroscopy has emerged as an important nondestructive technique since it allows us to look at the formulation without the

ACCEPTED MANUSCRIPT

interference of solvent molecules and thus probe the initial stage of the dissolution process, while giving information on short range interactions.(Ito et al, 2010); (Tres et al, 2015); (Yuan et al, 2015) In this context, the aim of the present work is to promote a deeper knowledge on PVP:PZQ formulations by using solid-state Nuclear Magnetic Resonance (NMR) and Differential Scanning Calorimetry (DSC) to demonstrate, for the first time, that solvent choice in the preparation of solid dispersions plays a crucial role in the physicochemical properties of the resulting formulations, as it can promote or inhibit PZQ crystallization.

2. MATERIALS AND METHODS

2.1 Materials.

Racemic Praziquantel ($C_{19}H_{24}N_2O_2$, purity > 99.4%) was purchased from Romikin (Buenos Aires, Argentina). Poly(vinylpyrrolidone) powder (K30, average MW 40,000) was purchased from BASF SE (Ludwigshafen, Germany). All the reagents and chemicals used for analytical purpose were of chromatography grade.

2.2 Preparation of Amorphous Praziquantel.

The PZQ sample was melted inside a stainless steel container in a vacuum oven for 3h at 150ºC. The melted sample was then rapidly cooled with liquid nitrogen to form an amorphous glass of PZQ that was kept at -10 °C (*circa* 50 °C bellow the glass transition temperature, T_g). It should be noted that under these conditions no decomposition of the sample was observed, either by DSC or NMR. This is in line with literature reports (El-Subbagh and Al-Badr, 1998) and was confirmed by LC-MS (96.8% *vs* 98.9% for the initial crystalline sample - see Appendix for more details).

ACCEPTED MANUSCRIPT

2.3 Preparation of Physical Mixtures.

Physical mixtures (PMs) of PVP and PZQ (150 mg), in 1:1, 2:1, and 3:1 weight ratios were prepared by physically mixing the components thoroughly for 10 min in a mortar until a homogeneous mixture was obtained. The powder was then passed through 100 mesh sieve and stored in a desiccator.

2.4 Preparation of Solid Dispersions.

I) Solid dispersions (SDs) of PVP:PZQ at 1:1, 2:1, and 3:1(w/w) were prepared by the solvent evaporation method. PZQ (150 mg) was dissolved in 10 ml of ethanol, and the polymer was dissolved in 10 ml of water. The solutions were mixed under magnetic stirring for 30 min. The solvents were then evaporated under reduced pressure, dried at 40 °C (48 h), passed through 100 mesh sieve and stored in a desiccator. II) Solid dispersions of PVP:PZQ at 1:1, 2:1 and 3:1 (w/w) were also prepared dissolving both components exclusively in ethanol using the same procedure as described in I).

2.5 Solubility Study.

Saturation solubility was determined by adding weighted amounts of the prepared PVP:PZQ PMs and SDs into 25-mL glass flasks containing distilled water (20 mL). All flasks were stoppered and kept shaking at 150 rpm for 72 h in a Boeco universal orbital shaker PSU-10i (Boeckel + Co, Hamburg, Germany) at 25 °C. The supernatant was then removed, filtered with Whatman filter paper (0.2 μm). The concentration of PZQ in solution was determined by UV analysis at 260 nm using a Boeco UV-visible spectrophotometer (Boeckel + Co, Hamburg, Germany). Experiments were performed in triplicate.

2.6 Differential Scanning Calorimetry (DSC) Experiments.

ACCEPTED MANUSCRIPT

DSC measurements were performed with a 2920MDSC system from TA Instruments Inc. Samples weighting between 3 to10 mg were placed into aluminum pans non-hermetically sealed. The measuring cell was continually purged with high purity helium gas at a flow rate of 30mL/min. An empty aluminum pan, identical to those used for the samples, was used as reference. The temperature and heat flow scales of the apparatus were performed as described.(Moura Ramos et al, 2004) The heat flow curves were obtained in the first ramp. The experimental protocol was as follow: a) PZQ sample was firstly equilibrated at -100˚C and then heated up to 165 ˚C, b) the PVP sample was equilibrated at 20 ˚C and heated up to 200 ºC, c) all the other samples were firstly equilibrated at -20 ˚C and then heated up to 210 ˚C. In all DSC runs a heating rate of 10 ºC/min was used. Cooling has been achieved with the liquid nitrogen cooling accessory (LNCA from TA) which provides automatic and continuous programmed sample cooling down. All the data were analyzed using TA Universal Analysis Software.

2.7 Solid-State NMR Experiments.

PZQ, PVP and samples containing both PZQ and PVP (~ 200 mg) were packed into 7 mm o.d. zirconia rotors, equipped with Kel-F caps. Samples with less than 200 mg (typically ~100 mg) were packed into a spherical Kel-F insert appropriate for a 7 mm o.d. zirconia rotor.^{13}C cross polarization/magic angle spinning (CP/MAS) spectra were obtained at 75.49 MHz, on a Tecmag Redstone/Bruker 300WB, with spinning rates of 3.1-4.2 kHz, unless otherwise stated. In these experiences, contact times of 3 ms and 90˚ RF pulses of around 4 μs were used. Relaxation delays were adjusted according to the PZQ sample under observation: crystalline and amorphous PZQ were measured with a delay of 20 s and 5 s, respectively. Whenever necessary, ^{13}C spinning sidebands were suppressed using the TOSS sequence (TOtal Suppression of Spinning Sidebands).(Dixon et al, 1982)

ACCEPTED MANUSCRIPT

Gaussian functions were selected to deconvolute relevant signals in ^{13}C CP/MAS spectra iteratively by the least-squares method using the software Origin (Microcal Software, Inc., USA).

^{13}C chemical shifts were referenced with respect to external glycine (^{13}CO observed at 176.03 ppm).

Proton relaxation times in the rotating frame ($^{H}T_{1\rho}$) were measured by recording the ^{13}C signal as a function of the ^{1}H spin-lock time (before cross-polarization), that was varied between 10 μs and 14 ms, in a total of 17 points. The spin-lock field B_1 used was 50 kHz. Spectra were run with 10 s recycle delay and a contact time of 400 μs (to minimize spin-diffusion during measurements). $^{H}T_{1\rho}$ values were determined via the Eq. 1:

$$M(t) = M_0 e^{-t/^{H}T_{1\rho}} \qquad \text{Eq. 1}$$

Eq. 1 was fitted to the experimental data (peak intensity as a function of ^{1}H spin-lock time), using the least-squares method. In this equation *M(t)* is the signal intensity at ^{1}H spin-lock time *t* and M_0 is the intensity when no ^{1}H spin-lock is used. Proton spin-lattice relaxation times ($^{H}T_1$) were measured under ^{13}C CP/MAS observation using the saturation recovery pulse sequence with TOSS.(Dixon et al, 1982) The 90° RF pulse duration was 4.4 μs, corresponding to a spin-lock RF field of about 46 kHz. The signal intensity from each carbon under study was plotted against recovery delay times t which were varied from 200 ms to 15 s (12 values) and the following equation was used to obtain the time constant $^{H}T_1$:

$$M(t) = M_0\left(1 - e^{-t/^{H}T_1}\right) \qquad \text{Eq. 2}$$

where *M(t)* is the signal intensity at the recovery delay time *t* and M_0 is the intensity when the recovery delay is zero. Either the software Origin (Microcal Software, Inc., USA) or the software available from Tecmag Inc. (Houston, USA) were used to do these fittings.

The relaxation measurements were always performed at 20 ˚C.

ACCEPTED MANUSCRIPT

2.8 Scanning Electron Microscopy (SEM).

Analysis of the samples by SEM was performed on a Hitachi S2400 equipment. Sample surfaces were previously sputtered with gold.

2.9 Thermal Gravimetric Analysis (TGA).

Combined TG-DSC measurements were carried out on a SETARAM TG-DTA 92 thermobalance under nitrogen atmosphere. Samples with mass in the range 26-35 mg were weighted on a platinum crucible and a heating rate of 5 K/min was used.

2.10 LC/MS of crystalline and amorphous PZQ samples

Methanolic solutions of PZQ (obtained from crystalline and amorphous PZQ) were analyzed on an LC/MS system with an HPLC Dionex Ultimate 3000 coupled in-line to a LCQ Fleet ion trap mass spectrometer equipped with an ESI ion source (Thermo Scientific). Separations were carried out with a Phenomenex Kinetix C18 (2) column (150 mm × 4,6 mm, 5 µm) at 35 ºC. An injection volume of 10 µL was delivered at a flow rate of 200 µLmin-1 using a linear gradient from 50 to 80 % in A - 0,1 % of formic acid in water (v/v) and B- acetonitrile, followed by a 4 min linear gradient to 100% acetonitrile, and then the column was requilibrated with 50 % of A for 10 min.

The mass spectrometer was operated in the ESI positive ion mode, with the following optimized parameters: ion spray voltage, +4.5 kV; capillary voltage, 16 V; tube lens offset, -63 V, sheath gas (N_2), 80 arbitrary units; auxiliary gas, 5 arbitrary units; capillary temperature, 300 ºC. Spectra typically correspond to the average of 20–35 scans, and were recorded in the range

ACCEPTED MANUSCRIPT

between 50-700 Da. Data acquisition and processing were performed using the Xcalibur software.

3. RESULTS AND DISCUSSION

3.1 Solubility Study.

The saturation solubility data of PZQ as a pure crystalline drug and in the corresponding PMs and SDs are shown in Table 1. As observed, the saturation solubility of PMs and SDs shows that PZQ solubility increases in the presence of PVP in comparison with the non-treated drug and that the higher the polymer content the more PZQ is dissolved, as reported by other authors, that tentatively explain the trend by the lowering of the surface tension of the medium in the presence of PVP which promotes a better wetting of the PZQ crystal surface.(de la Torre et al, 1999) Furthermore, SDs have higher saturation solubility than the corresponding PMs with the same PVP:PZQ ratio. In addition, SDs prepared from solutions with ethanol and water exhibit lower saturation solubility than their counterparts prepared exclusively in ethanol. The choice of solvent in the preparation of the different formulations appears to have some influence in solubility, which motivated the following NMR and DSC studies.

3.2 ^{13}C Solid-State NMR Spectroscopy and DSC of PMs.

The ^{13}C CP/MAS TOSS solid state NMR spectra of crystalline PZQ and PVP are depicted in Figure 2. Racemic PZQ crystallizes in the $P\bar{1}$ space group, with four molecules in the asymmetric unit.(Espinosa-Lara et al, 2013) Consistently, its ^{13}C CP/MAS TOSS solid-state

NMR spectrum shows more than 19 signals, the number of carbon nuclei in one molecule. A detailed discussion of this spectrum and its peak assignment (Table S1) was already published.(Arrúa et al, 2015) The ^{13}C CP/MAS TOSS solid-state NMR spectrum of PVP shows broad signals characteristic of an amorphous polymer. Peak assignment (Table S2, Appendix) was done taking into account the typical chemical shifts of the different type of carbon atoms present.

The ^{13}C CP/MAS TOSS spectra obtained from the physical mixtures (PVP:PZQ 1:1, 2:1 and 3:1, weight ratios) show no significant changes in both chemical shifts and line shape of the PZQ and PVP signals. These are a mere overlap of the spectra of the isolated components, with relative intensities reflecting the proportion of the two components. This result shows that grinding the two solids together neither destroys the crystalline structure of PZQ nor promotes the interaction between PZQ and the polymer.

Fig.2 Here

The solid-state NMR data are in agreement with the thermal analysis results. The DSC results confirm the chemical purity of the racemic crystalline sample: the obtained values for T_{onset}, T_{max} and enthalpy of fusion are, respectively, 138.16ºC, 142.52ºC and 94.19 J/g in agreement with the literature(El-Arini et al, 1998); (Passerini et al, 2006) and USP recommended melting range (136 – 142ºC). Although the physical mixtures showed a lower marginal shift (~ 2 ˚C) in the T_{max} of the melting point, this is not certainly related with a PVP-PZQ interaction because the onset temperature remains unchanged. As anticipated, it is also observed in the thermograms (Fig. 3) the lowering of the area of the endothermic peak ascribed to fusion of crystalline PZQ with the increase of polymer content. Using these enthalpic values, and assuming that no crystallization of the PZQ happens during the heating ramp, a rough estimation of the amount of crystalline

ACCEPTED MANUSCRIPT

PZQ in the samples can be done. For all PMs under investigation these estimates clearly indicate that the fractions of PZQ present in crystalline form are relatively high (Table 2). The decrease of the enthalpy value associated with the melt observed is a consequence of the dilution of crystalline PZQ in the binary sample and not due to the presence of amorphous PZQ. The broad endothermic curves at ~58 ºC correspond to a dehydration event of PVP, as reported by other authors.(Trastullo et al, 2015) The endothermic broad signals detected in the PVP sample were attributed to sample heterogeneity since consecutive assays showed similar peaks even with marginal shifts. We do not believe that the results of DSC (Fig. 3) clearly indicate that we are in presence of new polymorphic form or even a polymorphic transition. Our suspicion is based on: 1) the endothermic signal detected in the thermogram at ca. 80ºC is inside of a temperature region were the broad signal of the PVP K30 was observed; 2) no sequence of the intensity (and also peak definition) was visualized as the amount of PVP increases. Note that for the physical mixture (2:1) the peak at 80ºC is undiscernible.

Fig.3 here

3.3 ^{13}C Solid-State NMR Spectroscopy and DSC of SDs Obtained from Water and Ethanol Solutions.

Formulations prepared from mixing an ethanol solution of PZQ with an aqueous solution of PVP show differences not only in the overall solubility of PZQ (see Table 1) but also on their ^{13}C CP/MAS NMR spectra (Fig. 4, Table 3). Although crystalline PZQ is present in the sample, as attested by the resolution of the aromatic signals C7-C12 (120-140 ppm, Fig. 5), there is broadening of all the signals, consistent with the presence of some amorphous PZQ. The signal for C2 was deconvoluted to enhance those changes (Fig. 6, Table 4). Changes are also observed

ACCEPTED MANUSCRIPT

in the signals assigned to C3 (Fig. 5). No major changes were detected in the polymer signals (see Table S2, Appendix).

Fig.4 Here

Fig.5 Here

For crystalline PZQ, the ^{13}C CP/MAS C2 carbon signal is best described by two peaks, one centered at 161.71 ppm and the other at 164.07 ppm, corresponding to 66.9% and 25% of the peak area, respectively. The third peak at 165.22 ppm represents only 7.9% of the signal. For amorphous PZQ, these signals coalesce into one broad signal ($\Delta\nu_{½}$=257 Hz) at 164.36 ppm (Table 4).(Arrúa et al, 2015) In the spectra of the formulations prepared in a mixture of ethanol and water also two peaks are present. For all samples the chemical shifts of the two peaks are down-field shifted when compared to the values obtained for crystalline PZQ (approximately 161 and 163 ppm in the crystalline vs. 163 and165 ppm in the three samples), with no major difference in chemical shifts with the increase of PVP fraction. What is significant is that the difference in chemical shifts between the two peaks drops to half when PVP is present, which is consistent with the presence of amorphous PZQ (one signal at 164.4 ppm), that probably shifts the center of the two signals. The deconvolution of these signals (Fig. 6, Table 4) shows that both signals are, for the three samples, significantly wider than the corresponding signals for crystalline PZQ, attesting the presence of the amorphous form. The signal at circa 163 ppm becomes narrower with the increase in the amount of PVP, but the same cannot be said about the signal at 165 ppm, that becomes first wider and then narrower as the amount of PVP increases. Also, no trend is observed in the relative areas of both peaks. The amount of amorphous PZQ in these samples does not therefore correlate with the amount of PVP present. This is confirmed by

ACCEPTED MANUSCRIPT

the DSC thermograms that show the presence of crystalline PZQ (detection of an endothermic event attributed to fusion, see Fig. 7). The estimate of the amount of crystalline PZQ in the samples does not correlate with the amount of PVP present, as the samples 1:1 and 2:1 have the same amount of crystalline PZQ, which is significantly higher than the 3:1 sample (52%, vs. 20%, Table 2). The difference in saturation solubilities observed for the three samples appear to correlate solely with the amount of PVP present. The polymer promotes the wettability of the drug increasing its solubility, but the water content probably hampers the formation of an amorphous phase.

Fig.6 here

Fig.7 Here

3.4 ^{13}C Solid-State NMR Spectroscopy and DSC of SDs Obtained from Ethanol Solutions

PVP:PZQ 1:1 and 2:1 formulations prepared exclusively in ethanol have very different ^{13}C CP/MAS spectra from their counterparts prepared in a mixture of ethanol and water (Fig. 8). Their spectra are best described as the overlap of the spectra of amorphous PZQ with the spectrum of PVP, with no signs of crystalline PZQ. The difference is more evident in the aromatic signals, that collapse into two broad resonances, and in the signal attributed to C2 that is in these two spectra reduced to one broad signal at around 165 ppm, with $\Delta\nu_{½}$ of 282 and 291 Hz, respectively (Table 4, Fig.6). Relaxation measurements have shown PZQ and PVP miscibility in these solid dispersions (see next section) and the DSC results confirmed the

ACCEPTED MANUSCRIPT

absence of crystalline phase of PZQ since no endothermic event attributed to the melting was detected (Fig. 9).

The PVP:PZQ 3:1 formulation prepared from ethanol has an unexpected behavior as both its ^{13}C CP/MAS NMR spectrum and its DSC thermogram indicate the presence of crystalline PZQ. In the NMR spectrum, the signal attributed to C2 has clearly two components, centered at 161.9 and 164.9 ppm, with comparable widths to crystalline PZQ. The amount of crystalline PZQ (based on the DSC thermograms) show that this amount is higher than the one found in the sample with the same PVP:PZQ ratio prepared with two solvents (20% and 34%, respectively, see Table 2).

Fig.8 Here

Fig.9 Here

The presence of crystalline PZQ in the 3:1 formulation prepared in ethanol may be a result of the presence of water in the system introduced with the polymer, as the plasticization effect of water induces crystallization. PVP is hygroscopic, has several hydration shells,(Lebedeva et al, 03) and the water content is high. TGA analysis shows that the polymer contains about 15% of water in weight (see Appendix, Table S3). The same analysis shows that the amount of water present in the samples correlates solely with the amount of polymer (~9.5% and ~11% for 1:1 and 3:1 formulations, respectively), and not with the preparation method. It should be noted that this water content denotes the amount of water present in the final formulation and not the amount of water existent in the sample preparation. This does not explain however the higher amount of crystalline PZQ (Table 2) and its higher solubility (Table 1), when compared to its counterpart

ACCEPTED MANUSCRIPT

prepared in the binary mixture ethanol/water. One possibility is that crystal size and distribution throughout the sample (PVP:PZQ 3:1 prepared in ethanol) is different when compared to (PVP:PZQ 3:1 prepared in water/ethanol). With the objective to verify this hypothesis we analyzed the samples PVP:PZQ 2:1 prepared in ethanol and the samples PVP:PZQ 3:1 prepared in water and ethanol and only in ethanol with SEM as depicted in Figure 10. All samples, including the amorphous sample PVP:PZQ 2:1 prepared in ethanol, have crystals. For this sample however, the crystals are small and are individualized on the surface of an amorphous phase that constitutes the major component of the sample (Figures 10a-c). For the PVP:PZQ 3:1prepared in a mixture of solvents (Figures 10d-f), the particles are more heterogeneous, with clusters of crystals on the surface. The sample PVP:PZQ 3:1 prepared in ethanol (Figures 10g-i), has particles that resemble the ones found in the amorphous sample PVP:PZQ 2:1 prepared in ethanol as well as particles that resemble the ones found in the PVP:PZQ 3:1 prepared in a mixture of solvents with clusters of crystals on the surface and embedded on the amorphous phase. This intermediate nature probably accounts for the higher saturation solubility obtained with this sample when compared to its counterpart, prepared in a mixture of solvents.

Fig.10 Here

3.5 NMR Relaxation Studies on the Miscibility of Amorphous Solid Dispersions.

Solid-state NMR can probe miscibility in multicomponent solid dispersions at molecular level under a non-invasive mode.(Paudel et al, 2014); (Pham et al, 2010); (Yuan et al, 2014) While chemical shift changes and peak broadening are generally considered indications of

ACCEPTED MANUSCRIPT

drug/polymer chemical interactions subsequent to miscibility, molecular dynamics provide indirect evidence for phase homogeneity at the nanometric scale. Relaxation times enable evaluating mobility in different frequency ranges. Spin-lattice relaxation time (T_1) and spin-lattice relaxation time in the rotating frame ($T_{1\rho}$) depend on motions on the MHz and kHz scales, respectively. Hydrogen relaxation times (${}^{H}T_1$ and ${}^{H}T_{1\rho}$) are also strongly dependent on spin diffusion, an energy conservative process that may mask mobility data, due to both high isotopic natural abundance and gyromagnetic ratio of hydrogen nuclei. Spin diffusion involves magnetization transport (through the so-called “flip-flop” transitions) between dipolar interacting spin nuclei which then perform as a single spin reservoir characterized by averaged relaxation times. Typical time constants for proton spin flips are in the range 100 μs – 10 ms.(Koenig, 99) The longer the relaxation time the higher the probability of spin-diffusion to occur, i.e., ${}^{H}T_1$ will be more influenced by this process than ${}^{H}T_{1\rho}$. Hence, PZQ and PVP may each be considered a spin reservoir if a unique ${}^{H}T_1$ and/or ${}^{H}T_{1\rho}$ is measured, due to the averaging process over the entire molecule. Though adding a mechanism that may mask local motions, spin-diffusion can provide evidence for PVP:PZQ miscibility because the spin-diffusion rate are proportional to $1/d^6$, where d is the internuclear distance. Therefore, when the starting drug and polymer present different relaxation data, a single relaxation time measured for a solid dispersion indirectly shows that the drug and the polymer are miscible, because they behave as a single spin reservoir. ${}^{H}T_1$ and ${}^{H}T_{1\rho}$ enable detecting different miscibility scales. The equation that gives the distance of magnetization transfer within a molecule during *t* seconds is

$$M(t)^2 = 4Dt \qquad \text{Eq. 3}$$

ACCEPTED MANUSCRIPT

where D is the diffusion coefficient. For alkanes, for example, M(t) corresponds to 1.6, 7.0 and 50 nm for t equal to 1 ms, 20 ms and 1 s, respectively, considering that D is about 6.2×10^{-12} cm^2s^{-1}.(VanderHart and Khoury, 1984)

${}^{H}T_{1}$ values were obtained from PZQ, both as crystalline powder and also after amorphization (Tables 5 and 6). The proton spin-lattice relaxation rate for amorphous PZQ is about twice the corresponding value for crystalline PZQ. ${}^{H}T_{1}$ for pure PVP is about 1 s showing that the polymer relaxes faster than the amorphous drug (${}^{H}T_{1}$ of about 4 s). For solid dispersions 1:1 and 2:1 PVP:PZQ SDs prepared in ethanol, the results show that, within the error of the fitting, ${}^{H}T_{1}$ and ${}^{H}T_{1\rho}$ data are equivalent for PZQ and PVP (Table 6). These results are consistent with the drug and the polymer behaving as a unique spin reservoir and therefore as a single, homogeneous, phase. If the drug and the polymer chains are in close proximity, at a distance shorter than the length scale of proton spin diffusion, magnetization transfer from the slower to the faster relaxing spin reservoir is favored, and the relaxation times of both compound become equal to a weighted average of the values of the individual chains.(Bovey and Mirau, 96) The ratio of the molecular weights of PZQ and N-vinylpirrolidone (the precursor to PVP) is ca. 2.8 and the solid dispersion drug:carrier 1:1 (w/w) contains about 3 times more monomers than PZQ molecules. Therefore, evidence for PZQ and PVP miscibility would be obtaining ${}^{H}T_{1}$ and ${}^{H}T_{1\rho}$ of about 3.5 s and 19 ms, respectively. Experimental data were about 2 s and 10 ms (Table 6), that is about half of the ideal values. This discrepancy may be due to the presence of water because it induces a relaxation time decrease in PVP systems.(Sperger et al, 2011) It is worth mentioning that a similar effect was reported on the miscibility investigation and molecular mobility of nifedipine-PVP using ssNMR.(Yuan et al, 2014)

ACCEPTED MANUSCRIPT

The maximum effective spin-diffusion path length L for the protons to contact is given by(Douglass and Jones, 1966); (McBrierty and Douglass, 1981)

$$L^2 = 6W < w_0 >^2 d^2 t = 6\,Dt \qquad \text{Eq. 4}$$

where W is the transition probability per unit time that spins exchange energy, w_0 is the hydrogen Larmor frequency, d is the distance between hydrogen atoms, D is the spin diffusion coefficient determined by the average proton-to-proton distance and the strength of the dipolar interaction and t is the relaxation time, that is ${}^{H}T_1$ or ${}^{H}T_{1\rho}$. D is biased by molecular dynamics and therefore it is important to point out that NMR data were acquired at about 20 ˚C, that is below T_g for both PZQ and PVP (38 ˚C and 156 ˚C, respectively). Considering that D is of the order of 10^{-12} cm^2/s and that ${}^{H}T_1$ is about 2 s, the corresponding length scale for spin diffusion is 35 nm.(Douglass and Jones, 1966) Because ${}^{H}T_{1\rho}$ is about 11 ms, the length scale for spin diffusion is around 3 nm. Hence, PZQ and PVP are miscible in solid dispersion domains with a size larger than 3 nm.

4. CONCLUSIONS

The results presented here clearly show that for PVP:PZQ formulations the method of preparation has a significant influence in the saturation solubility of the drug. Samples prepared in the absence of solvent (PMs) are less soluble and their solid-state NMR spectra show that there is no interaction between the polymer and the drug. Samples prepared by dissolving the components, mixing and then removing the solvent (SDs) show different solubility extensions and interactions between PVP and PZQ that can be traced to the solvents used. The results show that higher ethanol content promotes the formation of a homogeneous phase that corresponds to both amorphous PVP and PZQ whereas higher water content stimulates PZQ crystallization. For

ACCEPTED MANUSCRIPT

samples with higher PZQ content prepared in ethanol, this translates into the preferential formation of a stable amorphous phase that contains the polymer and the drug and that clearly dominates the crystalline phase, which is still present, as attested by SEM, but in such a small amount that it is undetected both by solid-state NMR and DSC. Solid-state NMR relaxation studies have demonstrated that in these samples PZQ and PVP are miscible in a domain larger than 3 nm.

For samples with higher polymer content, the presence of water, introduced either by dissolving the polymer in water or via the polymer itself due to its high water content, induces PZQ crystallization. The major difference between the two 3:1solid dispersion samples studied appears to lie in the size of the crystals obtained and in the formation of crystal aggregates. The formulation prepared in ethanol has smaller aggregates and that likely accounts for the higher solubility observed for this sample.

What is curious is that, judging by the DSC results and by the solid-state NMR analysis of the samples prepared in ethanol and water and the 3:1 dispersion prepared in ethanol, the amount of crystalline phase formed does not directly correlate with the quantity of water present or the amount of PVP. The fraction of polymer present does directly correlate with saturation solubility possibly due to its effect on drug wettability and solubility. This is in fact seen in the amount of crystalline PZQ detected by DSC in the formulations prepared in ethanol and water and in the saturation solubility trends observed.

The choice of solvent in the preparation of PVP:PZQ SDs is therefore not an innocent one, as it can dramatically change the phase of the drug. The presence of water induces crystallization whereas the presence of ethanol promotes the formation of amorphous PZQ. A higher amorphous content does increase solubility but for these systems other factors have to be

ACCEPTED MANUSCRIPT

considered such as the amount of PVP present and the aggregation state of the crystalline material formed.

Acknowledgments

This work has been carried out with financial support from Fundação para Ciência e Tecnologia (FCT, Portugal, projects RECI/QEQ-QIN/0189/2012, UID/QUI/00100/2013, REM2013) and UNR (Argentina), CONICET (Argentina), MINCYT (Argentina) (PICT 1078). E.D.C. and M.J. F. are thankful to FCT for their fellowships (BL-CQE/2015-011 and RECI/QEQ-QIN/0189/2012, respectively) J.P thanks to CONICET (Argentina) for a Ph D. fellowship. The authors thank Dr. Isabel Nogueira (MicroLab – Electron Microscopy Laboratory at Instituto Superior Técnico) for recording the SEM images, Dr. Auguste Fernandes (CQE at IST) for the TGA measurements, and Dr. Conceição Oliveira and MSc Ana Dias (CQE at IST) for LC/MS studies.

Appendix - Supplementary data

Supplementary tables and an example of the calculation of the amount of crystalline PZQ in a binary mixture PZQ:PVP (1:1) by DSC, the DSC of amorphous PZQ and TGA results can be found in the Appendix.

ACCEPTED MANUSCRIPT

References

Arrúa,E.C., Ferreira,M.J., Salomon,C.J., Nunes,T.G., 2015. Elucidating the guest-host interactions and complex formation of praziquantel and cyclodextrin derivatives by 13C and 15N solid-state NMR spectroscopy. Int. J. Pharm., 496, 812-821.

Bagade,O., Shete,A., Dhole,S., Pujari,R., Raskar,V., Kharat,P., 2015. Design and statistical optimisation of praziquantel tablets by using solid dispersion approach. Asian J. Pharm., 9, 83-92.

Baghel,S., Cathcart,H., O'Reilly,N.J., 2016. Polymeric Amorphous Solid Dispersions: A Review of Amorphization, Crystallization, Stabilization, Solid-State Characterization, and Aqueous Solubilization of Biopharmaceutical Classification System Class II Drugs. J. Pharm. Sci. , in press (doi:10. 1016/j. xphs. 2015. 10. 008).

Baird,J.A., Taylor,L.S., 2012. Evaluation of amorphous solid dispersion properties using thermal analysis techniques. Adv. Drug Delivery Rev., 64, 396-421.

Bovey,F.A., Mirau,P.A., 1996. NMR of Polymers. Academic Press.

CDC, 7-11-2012.Centers for Disease Control and Prevention. Parasites - Schistosomiasis. Treatment.http://www.cdc.gov/parasites/schistosomiasis/treatment.html (accessed 13.06.16)

Chaves,I.S., Rodrigues,S.G., Melo,N.F.S., de Jesus,M.B., Fraceto,L.F., de Paula,E., Pinto,L.M.A., 2010. Alternatives for treatment of schistosomiasis: Physicochemical

ACCEPTED MANUSCRIPT

characterization of inclusion complex between praziquantel and hydroxypropyl-β-cyclodextrin. Lat. Am. J. Pharm., 29, 1067-1074.

de la Torre,P., Torrado,S., Torrado,S., 1999. Preparation, Dissolution and Characterization of Praziquantel Solid Dispersions. Chem. Pharm. Bull., 47, 1629-1633.

Dixon,W.T., Schaefer,J., Sefcik,M.D., Stejskal,E.O., McKay,R.A., 1982. Total suppression of sidebands in CPMAS C-13 NMR. J. Magn. Reson., 49, 341-345.

Douglass,D.C., Jones,G.P., 1966. Nuclear Magnetic Relaxation of n-Alkanes in the Rotating Frame. J. Chem. Phys., 45, 956.

El-Arini,S.K., Giron,D., Leuenberger,H., 1998. Solubility Properties of Racemic Praziquantel and Its Enantiomers. Pharm. Dev. Technol., 3, 557-564.

El-Subbagh,H.I., Al-Badr,A.A., 1998. Praziquantel. Analytical Profiles of Drug Substances and Excipients, 25, 463-500.

Espinosa-Lara,J.C., Guzman-Villanueva,D., Arenas-García,J.I., Herrera-Ruiz,D., Rivera-Islas,J., Román-Bravo,P., Morales-Rojas,H., Höpfl,H., 2013. Cocrystals of Active Pharmaceutical Ingredients – Praziquantel in Combination with Oxalic, Malonic, Succinic, Maleic, Fumaric, Glutaric, Adipic, And Pimelic Acids. Cryst. Growth Des., 13, 169-185.

ACCEPTED MANUSCRIPT

Fonseca,L.B., Nele,M., Volpato,N.M., Seiceira,R.C., Pinto,J.C., 2013. Production of PMMA Nanoparticles Loaded with Praziquantel Through In Situ Miniemulsion Polymerization. Macromol. React. Eng., 7, 54-63.

Frezza,T.F., Gremião,M.P.D., Zanotti-Magalhães,E.M., Magalhães,L.A., de Souza,A.L.R., Allegretti,S.M., 2013. Liposomal-praziquantel: Efficacy against Schistosoma mansoni in a preclinical assay. Acta Trop., 128, 70-75.

Haaf,F., Sanner,A., Straub,F., 1985. Polymers of N-Vinylpyrrolidone: Synthesis, Characterization and Uses. Polym. J., 17, 143-152.

Ito,A., Watanabe,T., Yada,S., Hamaura,T., Nakagami,H., Higashi,K., Moribe,K., Yamamoto,K., 2010. Prediction of recrystallization behavior of troglitazone/polyvinylpyrrolidone solid dispersion by solid-state NMR. Int. J. Pharm., 383, 18-23.

Koenig,J.L., 1999. Spectroscopy of Polymers. Elsevier.

LaFountaine,J.S., McGinity,J.W., Williams,R.O., 2016. Challenges and Strategies in Thermal Processing of Amorphous Solid Dispersions: A Review. AAPS PharmSciTech, 17, 43-55.

Lebedeva,T.L., Kuptsov,S.A., Feldctein,M.M., Plate,N.A., 2003. Molecular Arrangement of Water Associated with Poly(N-vinyl pyrrolidone) in the First Hydrate Shell. Nova Science Publishers, Inc United States, New York, 69-93.

ACCEPTED MANUSCRIPT

Lindenberg,M., Kopp,S., Dressman,J.B., 2004. Classification of orally administered drugs on the World Health Organization Model list of Essential Medicines according to the biopharmaceutics classification system. European Journal of Pharmaceutics and Biopharmaceutics, 58, 265-278.

Malhado,M., Pinto,D.P., Silva,A.C.A., Silveira,G.P.E., Pereira,H.M., Santos,J.G.F., Jr., Guilarducci-Ferraz,C.V.V., Vicosa,A.L., Nele,M., Fonseca,L.B., Pinto,J.C., Calil-Elias,S., 2016. Preclinical pharmacokinetic evaluation of praziquantel loaded in poly (methyl methacrylate) nanoparticle using a HPLC-MS/MS. J. Pharm. Biomed. Anal., 117, 405-412.

McBrierty,V.J., Douglass,D.C., 1981. Recent advances in the NMR of solid polymers. J. Polym. Sci. Macromol. Rev., 16, 295-366.

Meyer,T., Sekljic,H., Fuchs,S., Bothe,H., Schollmeyer,D., Miculka,C., 2009. Taste, A New Incentive to Switch to (*R*)-Praziquantel in Schistosomiasis Treatment. PLoS. Negl. Trop. Dis., 3, e357.

Moura Ramos,J.J., Taveira-Marques,R., Diogo,H.P., 2004. Estimation of the fragility index of indomethacin by DSC using the heating and cooling rate dependency of the glass transition. J. Pharm. Sci., 93, 1503-1507.

Newman,A., Engers,D., Bates,S., Ivanisevic,I., Kelly,R.C., Zografi,G., 2008. Characterization of amorphous API:Polymer mixtures using X-ray powder diffraction. J. Pharm. Sci., 97, 4840-4856.

ACCEPTED MANUSCRIPT

Passerini,N., Albertini,B., Perissutti,B., Rodriguez,L., 2006. Evaluation of melt granulation and ultrasonic spray congealing as techniques to enhance the dissolution of praziquantel. Int. J. Pharm., 318, 92-102.

Patra,M., Ingram,K., Leonidova,A., Pierroz,V., Ferrari,S., Robertson,M.N., Todd,M.H., Keiser,J., Gasser,G., 2013. In Vitro Metabolic Profile and in Vivo Antischistosomal Activity Studies of (η6-Praziquantel)Cr(CO)3 Derivatives. J. Med. Chem., 56, 9192-9198.

Paudel,A., Geppi,M., Van den Mooter,G., 2014. Structural and Dynamic Properties of Amorphous Solid Dispersions: The Role of Solid-State Nuclear Magnetic Resonance Spectroscopy and Relaxometry. J. Pharm. Sci., 103, 2635-2662.

Pham,T.N., Watson,S.A., Edwards,A.J., Chavda,M., Clawson,J.S., Strohmeier,M., Vogt,F.G., 2010. Analysis of Amorphous Solid Dispersions Using 2D Solid-State NMR and 1H T1 Relaxation Measurements. Mol. Pharmaceutics, 7, 1667-1691.

Sperger,D.M., Fu,S., Block,L.H., Munson,E.J., 2011. Analysis of composition, molecular weight, and water content variations in sodium alginate using solid-state NMR spectroscopy. J. Pharm. Sci., 100, 3441-3452.

Tatton,A.S., Pham,T.N., Vogt,F.G., Iuga,D., Edwards,A.J., Brown,S.P., 2013. Probing Hydrogen Bonding in Cocrystals and Amorphous Dispersions Using 14N−1H HMQC Solid-State NMR. Mol. Pharm., 10, 999-1007.

ACCEPTED MANUSCRIPT

Trastullo,R., Dolci,L.S., Passerini,N., Albertini,B., 2015. Development of flexible and dispersible oral formulations containing praziquantel for potential schistosomiasis treatment of pre-school age children. Int. J. Pharm., 495, 536-550.

Tres,F., Coombes,R.S., Phillips,R.A., Hughes,P.L., Wren,A.S., Aylott,W.J., Burley,C.J., 2015. Investigating the Dissolution Performance of Amorphous Solid Dispersions Using Magnetic Resonance Imaging and Proton NMR. Molecules, 20, 16404-16418.

VanderHart,D.L., Khoury,F., 1984. Quantitative determination of the monoclinic crystalline phase content in polyethylene by 13C n.m.r. Polymer, 25, 1589-1599.

WHO, 2016a.World Health Organization. Media Center. Schistosomiasis.http://www.who.int/mediacentre/factsheets/fs115/en/ (accessed 13.06.16)

WHO, 2016b.World Health Organization. Schistosomiasis. Strategy.http://www.who.int/schistosomiasis/strategy/en/ (accessed 13.06.16)

Yuan,X., Sperger,D., Munson,E.J., 2014. Investigating Miscibility and Molecular Mobility of Nifedipine-PVP Amorphous Solid Dispersions Using Solid-State NMR Spectroscopy. Mol. Pharmaceutics, 11, 329-337.

Yuan,X., Xiang,T.X., Anderson,B.D., Munson,E.J., 2015. Hydrogen Bonding Interactions in Amorphous Indomethacin and Its Amorphous Solid Dispersions with Poly(vinylpyrrolidone) and Poly(vinylpyrrolidone-co-vinyl acetate) Studied Using 13C Solid-State NMR. Mol. Pharm., 12, 4518-4528.

ACCEPTED MANUSCRIPT

Figure Captions:

Figure 1. Molecular formulas of PZQ and PVP, with the numbering scheme adopted. The * in C3 of PZQ denotes the chiral center.

Figure 2. ^{13}C CP/MAS TOSS NMR spectra of crystalline PZQ, PVP and PMs PVP:PZQ.

Figure 3. DSC thermograms of PVP, PZQ and the PMs obtained after previous sample temperature equilibration.

Figure 4. ^{13}C CP/MAS TOSS NMR spectra of crystalline and amorphous PZQ, PVP and the PVP:PZQ SDs prepared from ethanol and water.

Figure 5. ^{13}C CP/MAS TOSS NMR sub-spectra of crystalline and amorphous PZQ, PVP and the PVP:PZQ SDs prepared from ethanol and water, showing the signals for carbonyl C2, aromatic carbons (C7-C12) and C3 (from left to right).

Figure 6. ^{13}C CP/MAS NMR spectra of the C2 carbon in PVP:PZQ SDs prepared from ethanol and water (W/E) and only from ethanol (E/E) (the black lines represent the experimental spectra, the green lines (or striped lines in the printed version) represent the fitted Gaussian functions used in deconvolutions, the red lines (or checkered lines in the printed version) show the cumulative fitting curve and the blue lines (or grey full lines in the printed version) represent the regular residual of the fitting).

Figure 7. DSC thermograms of PVP, PZQ and the SDs prepared with ethanol and water. The experimental DSC protocol includes in the first step the sample temperature equilibration.

ACCEPTED MANUSCRIPT

Figure 8. ^{13}C CP/MAS NMR Spectra of the C2 carbon in PVP:PZQ SDs prepared from ethanol.

Figure 9. DSC thermograms of PVP, PZQ and SDs prepared with ethanol. The experimental DSC protocol includes in the first step the sample temperature equilibration.

Figure 10. SEM of a) SD PVP:PZQ 2:1 E/E with 100× magnification, b) SD PVP:PZQ 2:1 E/E with 750× magnification; c) SD PVP:PZQ 2:1 E/E with 3000× magnification, d) SD PVP:PZQ 3:1 W/E with 100× magnification, e), SD PVP:PZQ 3:1 W/E with 3000× magnification, f) SD PVP:PZQ 3:1 W/E with 15000× magnification g) SD PVP:PZQ 3:1 E/E with 100× magnification, h) SD PVP:PZQ 3:1 E/E with 1300× magnification, i) SD PVP:PZQ 3:1 E/E with 3500× magnification.

ACCEPTED MANUSCRIPT

Figure 1

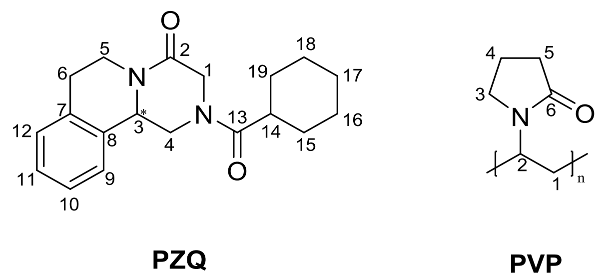

Figure 2

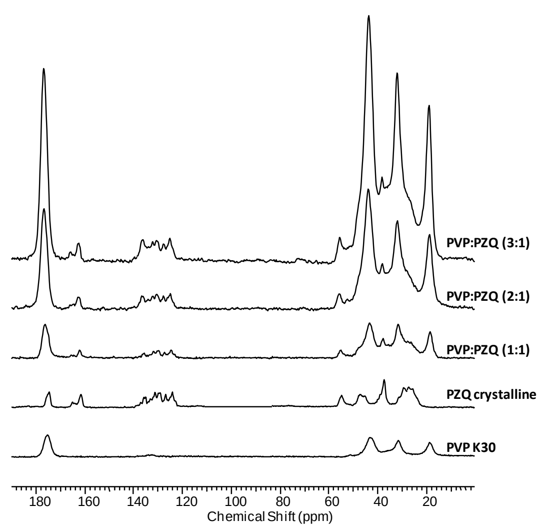

Figure 3

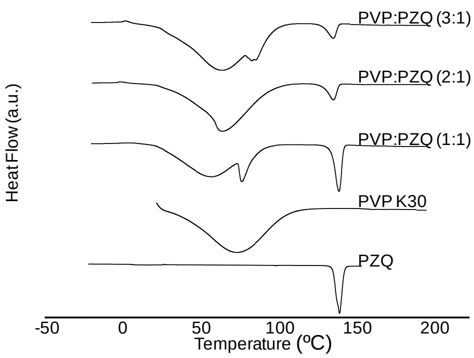

Figure 4

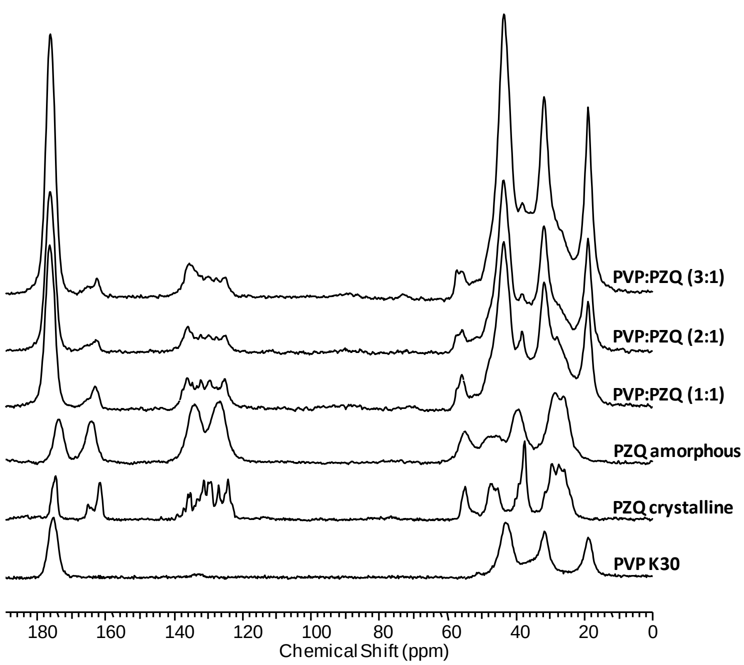

Figure 5

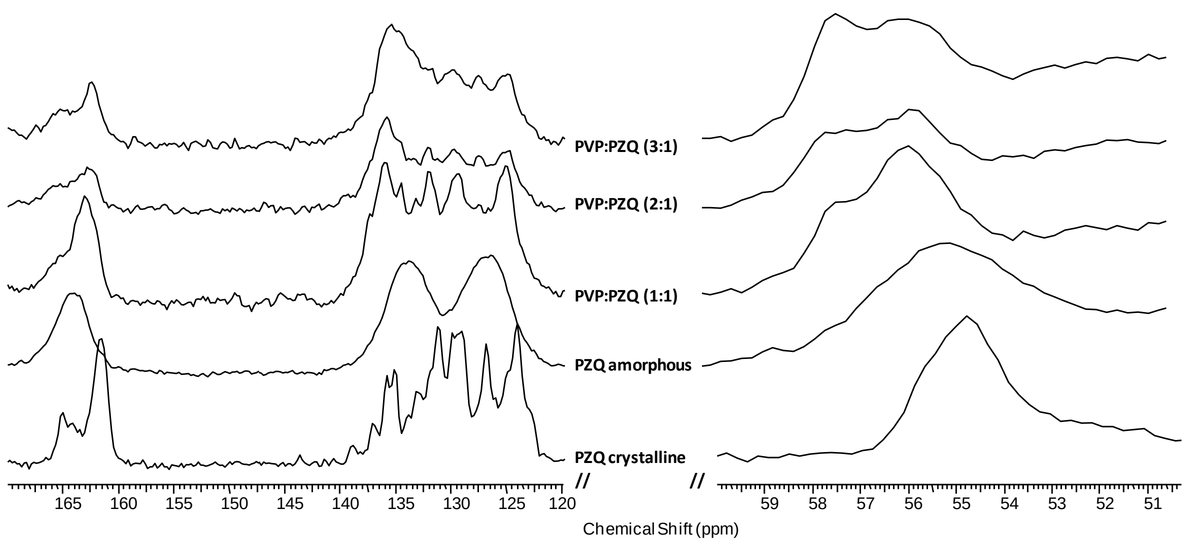
PVP:PZQ (3:1)
PVP:PZQ (2:1)
PVP:PZQ (1:1)
PZQ amorphous
PZQ crystalline
165 160 155 150 145 140 135 130 125 120
59 58 57 56 55 54 53 52 51
Chemical Shift (ppm)

ACCEPTED MANUSCRIPT

Figure 6 in color

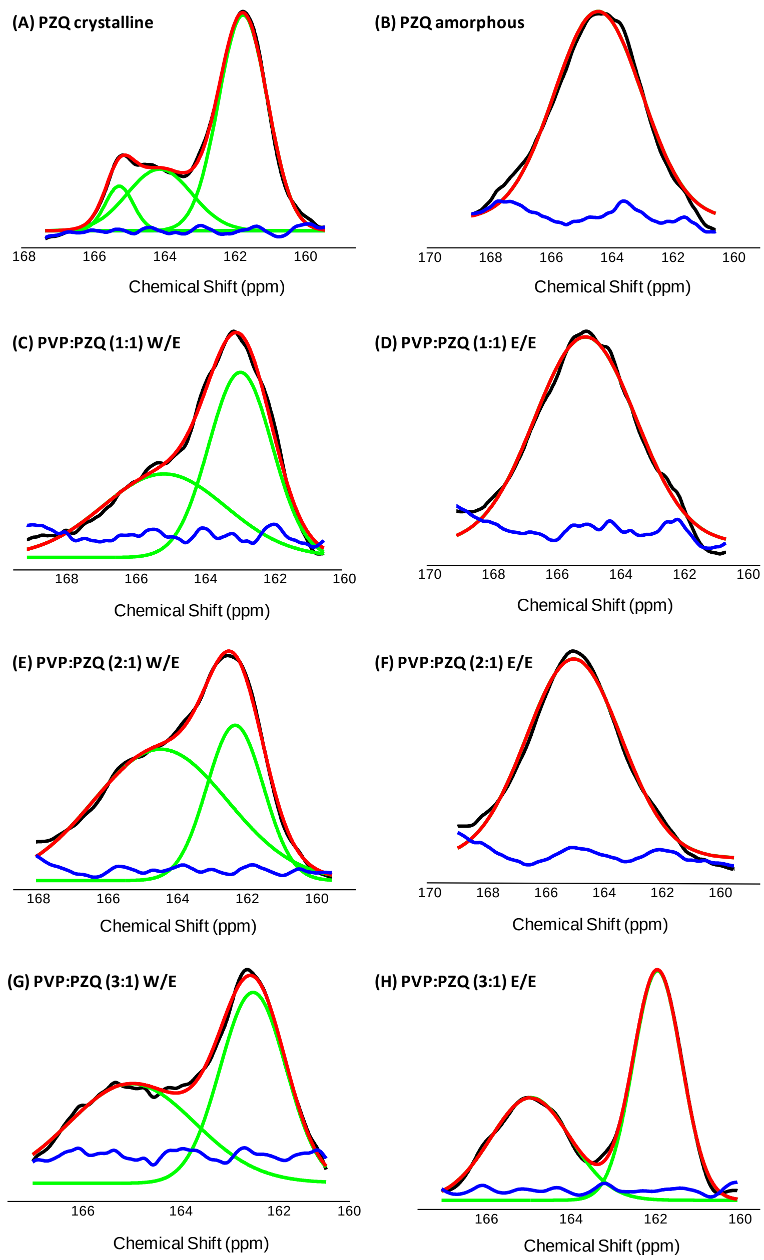

Figure 7

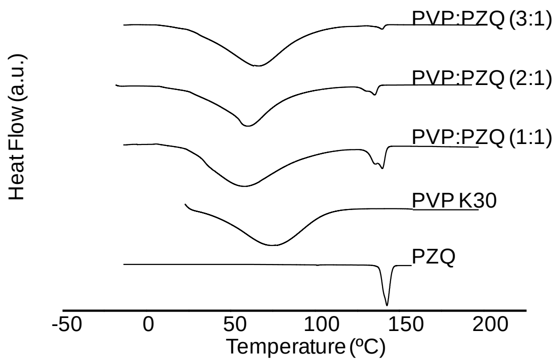

Figure 8

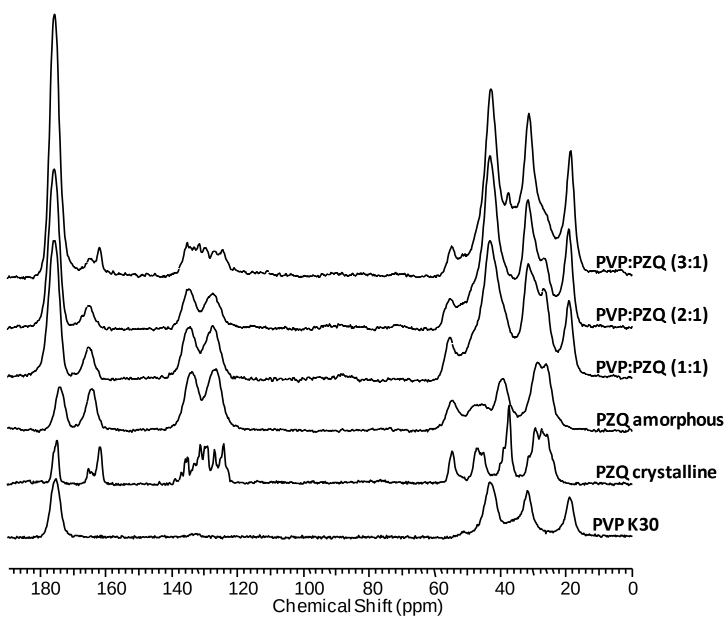

Figure 9

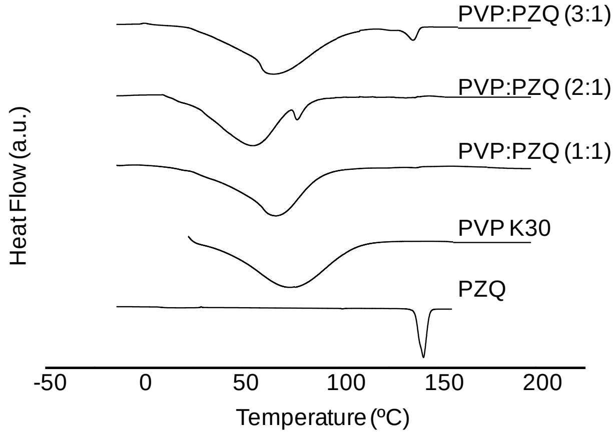

Figure 10

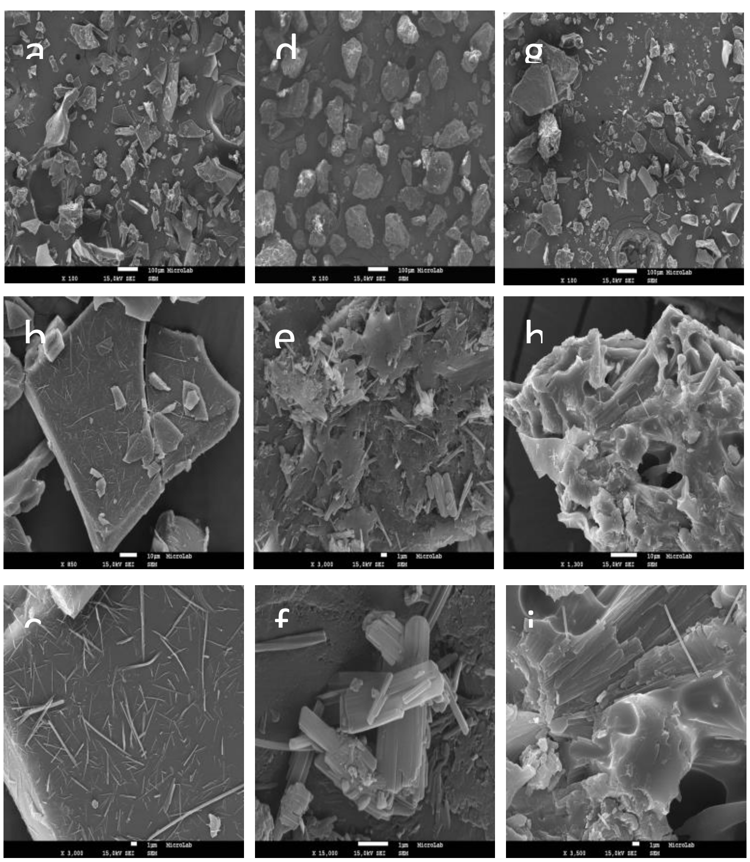

ACCEPTED MANUSCRIPT

Table 1. Saturation solubility of PZQ

Sample	Solvent	PVP:PZQ ratio (w/w)	Saturation solubility (mg/mL)
PZQ	--	--	0.31±0.01
PVP:PZQ (PM)	--	1:1	0.49±0.03
PVP:PZQ (PM)	--	2:1	0.62±0.02
PVP:PZQ (PM)	--	3:1	0.74±0.06
PVP:PZQ (SD)	Ethanol-Water	1:1	0.78±0.02
PVP:PZQ (SD)	Ethanol-Water	2:1	0.90±0.08
PVP:PZQ (SD)	Ethanol-Water	3:1	1.15±0.02
PVP:PZQ (SD)	Ethanol	1:1	1.08±0.04
PVP:PZQ (SD)	Ethanol	2:1	1.17±0.03
PVP:PZQ (SD)	Ethanol	3:1	1.29±0.03

Table 2. Melting temperature, enthalpy of fusion and estimation of the amount of crystalline PZQ (PZQ cryst.,%) in PMs and SDs

	Crystalline PZQ	**PM**			**SD (water/ethanol)**			**SD (ethanol)**		
		1:1	**2:1**	**3:1**	**1:1**	**2:1**	**3:1**	**1:1**	**1:2**	**3:1**
T_m (°C)	142.52	140.35	137.04	136.58	139.94	139.71	139.91	[b]	[b]	137.08
ΔH(J/g)	94.19	39.29	21.47	17.06	24.70	16.24	4.77	[b]	[b]	8.06
%PZQ cryst.[a]	-	~83	~68	~72	~52	~52	~20	0	0	~34

[a]Estimated taking into account the area of the crystalline peak in the thermograms (for more details see Appendix).

[b]Not detected in the thermogram

ACCEPTED MANUSCRIPT

Table 3. ^{13}C CP/MAS NMR chemical shifts (δ/ppm) of pure PZQ, both in the crystalline and amorphous forms, and in solid dispersions prepared from: ethanol and water (E/W) or only ethanol (E/E).

C	PZQ[a] (crystalline)	PZQ[a] (amorphous)	PZQ:PVP 1:1 SD(E/W)	PZQ:PVP 1:2 SD(E/W)	PZQ:PVP 1:3 SD(E/W)	PZQ:PVP 1:1 SD(E/E)	PZQ:PVP 1:2 SD(E/E)	PZQ:PVP 1:3 SD(E/E)
1	47.30	47.29	*	*	*	*	*	*
2	161.706[b], 164.07[b], 165.22[b]	164.36[b]	162.94[b],165.15[b]	162.292[b], 164.44[b]	162.495[b], 164.97[b]	165.00[b]	164.95[b]	161.904[b], 164.906[b]
3	54.92, 55.80	54.95	55.57, 57.09	55.57, 56.87	57.34, 56.25	55.35	55.57	54.70
4	45.56	47.29	*	*	*	*	*	*
5	40.30,39.24, 37.50	39.7	37.92*	38.14*	37.92*	*	*	37.49
6	27.48	28.34	27.90*	27.25*	*	26.81*	26.20*	*
7	135.30, 135.96	134.42	135.95	135.73	135.29	134.70	134.64	135.07
8	131.38	134.42	131.81	132.02	131.59	134.70	134.64	131.37
9	127.02	127.45	127.45	127.45	127.45	127.23	127.23	126.80
10	124.19	127.45	125.05	124.62	124.84	127.23	127.23	124.18
11	129.20	127.45	129.41	129.63	129.63	127.23	127.23	129.633
12	130.07	134.42	-	-	-	134.70	134.64	-
13	174.67, 175.30, 175.73	174.50	*	*	*	*	*	*
14	40.30,39.24, 37.50	39.70	37.92	38.14	37.92	*	*	37.49*
15	31.62	28.34	*	*	*	*	*	*
16	24.43	28.34	*	*	*	26.81*	26.60*	*
17	26.82	28.34	26.81*	*	*	26.81*	26.60*	*
18	25.74	28.34	*	*	*	26.81*	26.60*	*
19	29.43	28.34	*	*	*	*	*	*

*PZQ resonance overlaps with PVP signals.

[a] (Arrúa et al, 2015)

[b] Values obtained from the deconvolution of the signal

ACCEPTED MANUSCRIPT

Table 4. Parameters used to fit Gaussian functions to the PZQ C2 carbon signals obtained from ^{13}C CP/MAS spectra of crystalline and amorphous PZQ and PVP:PZQ SDs.

	δ (ppm)	**Width (Hz)**	**Peak Area (%)**
PZQ crystalline	161.706±0.003	123.8±0.8	66.9±0.3
	164.07±0.03	162±5	25±1
	165.22±0.01	71±2	7.9±0.7
PZQ amorphous	164.36±0.01	257±2	100
PVP:PZQ (W/E)			
1:1	162.94±0.01	163±2	53±3
	165.2±0.1	317±20	47±5
2:1	162.292±0.003	144±2	33±1
	164.44±0.05	343±10	67±3
3:1	162.495±0.005	119.3±0.8	50.1±0.7
	164.97±0.01	227±4	50±1
PVP:PZQ (E/E)			
1:1	165.00±0.01	282±2	100
2:1	164.95±0.01	291±2	100
3:1	161.904±0.001	102±3	57.8±0.2
	164.906±0.004	167.6±0.8	42.1±0.4

ACCEPTED MANUSCRIPT

Table 5. Proton spin-lattice relaxation time ($^{H}T_1$, s) obtained for crystalline PZQ. The errors associated with the fittings are also shown.

C2 (δ/ppm)	C3	C14,5	C7,8,12,9,10,11	C13
8.89±0.69 (164) 9.35±0.75 (161)	7.76±0.19	7.77±0.11	7.54±0.08*	8.08±0.19

*obtained from the center of the multiple peaks.

Table 6. Proton spin-lattice relaxation time ($^{H}T_1$, s) and spin-lattice relaxation time in the rotating frame ($^{H}T_{1\rho}$, ms) obtained for amorphous PZQ, PVP and PVP:PZQ (1:1 and 2:1) SDs. The errors associated with the fittings are also shown.

	Amorphous PZQ						PVP			
	$^{H}T_1$(s)									
	C2	C3	C14,5	C7,8,12	C9,10,11	C13	C1,5	C2,3	C4	C6
Pure	3.96±0.12	4.17±0.31	4.36±0.29	4.10±0.21	4.46±0.25	4.03±0.20	0.96±0.04	0.93±0.04	0.89±0.04	0.96±0.03
PVP:PZQ (1:1)	2.08±0.09	1.85±0.20	&	2.07±0.10	2.13±0.08	1.85±0.08*	2.01±0.05	1.85±0.07	1.79±0.09	1.85±0.08*
PVP:PZQ (2:1)	2.22±0.11	2.28±0.14	&	2.39±0.11	2.12±0.13	2.16±0.02*	2.09±0.04	2.17±0.04	1.93±0.06	2.16±0.02*
	$^{H}T_{1p}$(ms)									
	C3						C4			
Pure	9.73±0.98						15.42±0.90			
PVP:PZQ (1:1)	11.20±0.68						10.12±0.20			
PVP:PZQ (2:1)	11.27±1.26						10.09±0.15			

* obtained from carbonyl PVP and PZQ overlapping signals.
& unresolved signal.